First-principles study of carrier-induced ferromagnetism in bilayer and multilayer zigzag graphene nanoribbons

メタデータ	言語: eng
	出版者:
	公開日: 2022-03-10
	キーワード (Ja):
	キーワード (En):
	作成者:
	メールアドレス:
	所属:
URL	https://doi.org/10.24517/00065555

First-principles study of carrier-induced ferromagnetism in bilayer and multilayer zigzag graphene nanoribbons

Keisuke Sawada, Fumiyuki Ishii and Mineo Saito

View Online   Export Citation   CrossMark

ARTICLES YOU MAY BE INTERESTED IN

First-principles study of carrier-induced ferromagnetism in bilayer and multilayer zigzag graphene nanoribbons

Keisuke Sawada,[1] Fumiyuki Ishii,[2,a] and Mineo Saito[2,3]

[1]*Department of Applied Physics, The University of Tokyo, Hongo, Tokyo 113-8656, Japan*
[2]*Faculty of Mathematics and Physics, Institute of Science and Engineering, Kanazawa University, Kanazawa 920-1192, Japan*
[3]*Collaborative Research Center for Frontier Simulation Software for Industrial Science, Institute of Industrial Science, University of Tokyo, 4-6-1 Komaba, Meguro-ku, Tokyo 153-8503, Japan*

We studied magnetism in bilayer and multilayer zigzag graphene nanoribbons (ZGNRs) through first-principles density functional theory calculations. We found that the magnetic ground state of bilayer ZGNRs is the C-type antiferromagnetic (AFM) state, which is the AFM order between intraplane-edge carbon atoms and ferromagnetic (FM) order between interplane edge carbon atoms. In the cases of infinitely stacked multilayer ZGNRs, i.e., zigzag graphite nanoribbons, the C-type AFM state is also the most stable. By carrier doping, we found that the magnetic ground state changed from the C-AFM state to the FM state and, thus, realized two-dimensional FM surface (edge) states of graphite with a metallic conductivity. © 2014 AIP Publishing LLC. [http://dx.doi.org/10.1063/1.4870766]

Nano spintronics applications are considered to be among many useful applications of graphenes. Spin transport has been experimentally observed using single graphene layers,[1,2] and a half-metallic property has been theoretically predicted for nano-graphenes.[3–5] Zigzag graphene nanoribbons (ZGNRs) have attracted scientific interest owing to their magnetic properties originating from edge states. Fujita *et al.* clarified that ZGNRs have flat-electron bands and suggested that their ground states have an antiferromagnetic (AFM) state.[6,7] Carrier doping leads to the noncollinear magnetic state and the parallel interedge spin state accompanied by the parallel configuration of the two ferromagnetic (FM) chains located at both edges.[8] Moreover, band gaps can be changed by tuning edge spin directions in noncollinear magnetic ZGNR.[9]

Some magnetic device applications require ZGNR to have a large magnetization and an FM ground state. We predict that the FM ground state is achieved by carrier doping. The construction of multilayer ZGNRs by stacking ZGNR layers is one effective approach to increase the magnetization. Lee *et al.* reported on first-principles studies of the edge magnetism in stacked ZGNR layers and predicted that the FM coupling between neighboring ZGNR layers is energetically favorable.[10,11] However, they only considered ZGNR with FM configuration between intraplane edges. It is expected that bilayer or multilayer ZGNRs will have a variety of magnetic configurations that monolayer ZGNRs do not. Therefore, it is imperative that we investigate the magnetic structures of multilayer ZGNRs to understand the energetics in stacked ZGNRs.

In this study, we performed first-principles total-energy calculations on bilayer and multilayer ZGNRs and clarify that stacked ZGNRs show a variety of magnetic structures. We found that the magnetic ground state is an AFM structure having AFM coupling between intraplane edges and FM coupling between interplane edges [Fig. 2(c)]. The FM ground state was realized by carrier doping in bilayer as well as monolayer ZGNRs.

Using OPENMX code,[12] we performed first-principles electronic-structure calculations based on the density-functional theory (DFT). An exchange correlation potential was evaluated via a generalized gradient approximation.[13] A norm-conserving pseudopotential method[14] was used, and the wave functions were expanded by a linear combination of multiple pseudo-atomic orbitals (LCPAO).[15,16] Two valence orbitals (s- and p-orbitals) without a polarization orbital (d-orbital) for C atoms and a single valence orbital (s-orbital) with a polarization orbital (p-orbital) for H atoms were used as the basis set. We used a repeated slab model (Fig. 1) in which the length of a vacuum region along the non-periodic direction (y-, z-directions) was larger than 10 Å, and the lattice constant along the periodic direction
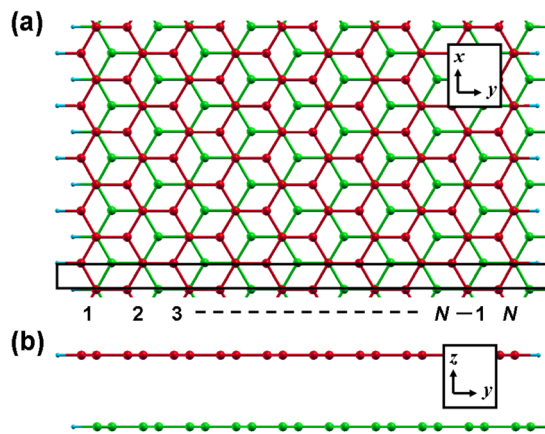
FIG. 1. Atomic structure of bilayer ZGNR. The large and small spheres denote C and H atoms, respectively. The red and green colors indicate the top and bottom ZGNR layers, respectively. The rectangle with solid lines indicates a unit cell. N is the width of the ZGNR. This figure shows the ZGNR with $N = 10$. (a) and (b) show the xy- and yz-planes, respectively.

a)Electronic mail: fishii@mail.kanazawa-u.ac.jp
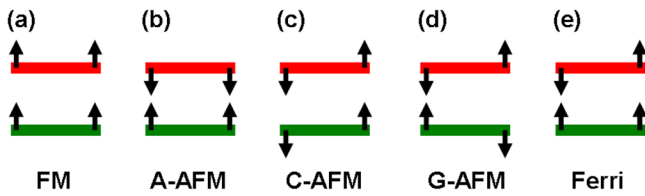
FIG. 2. Magnetic structures of bilayer ZGNR. The red and green rectangles denote the top and bottom ZGNR layers, respectively. The arrows represent the spin directions at edges. (a) denotes the ferromagnetic configuration. (b)–(d) denote the antiferromagnetic configuration. (e) denotes the ferrimagnetic configuration.

TABLE I. The calculated total energy difference from the ground state and indirect band gap of several magnetic states in bilayer ZGNR.

Magnetic states	ΔE (meV/layer)	Band gap (eV)
NM	83.5	0.0
FM	5.1	0.0
A-AFM	6.6	0.15
C-AFM	0.0	0.38
G-AFM	5.2	0.13
Ferri	4.9	0.0

(x-direction) (2.46 Å) was deduced from the experimental value observed for graphite. We sampled $60\,k$ points in the periodic direction (x-direction). The magnetic moment for each atom was estimated by a fuzzy cell partitioning method.[17] The AB-stacking structure for the bilayer ZGNR was used, and the interlayer distance d between the ZGNR and graphene was 3.35 Å, which was taken to be the same as the experimental interlayer distance of graphite.

We considered a bilayer ZGNR with ribbon width $N = 10$. The bilayer ZGNR has several possible collinear magnetic structures, whereas the monolayer ZGNR shows only two collinear magnetic structures, with the FM and AFM spin order between both edges. We used the notation of magnetic structures following to the perovskite manganite. Perovskite manganite, $La_{1-x}Sr_xMnO_3$, has several magnetic ground state by carrier-doping:[18–20] FM, A-type (interplane AFM and intraplane FM orders), C-type (interplane FM and intraplane AFM orders), and G-type (interplane AFM and intraplane AFM orders) AFM states. By emulating $La_{1-x}Sr_xMnO_3$, we considered the FM, A-AFM, C-AFM, G-AFM, and Ferrimagnetic (Ferri) states in the bilayer ZGNR, as shown in Fig. 2. Table I shows the total energy difference per ZGNR
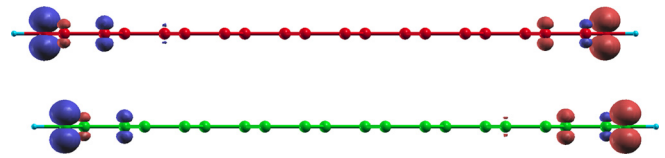
FIG. 4. Spin density of bilayer ZGNR for the C-AFM state. The red and blue isosurfaces denote the up and down spin states, respectively. The isovalues are 0.008 e/Bohr^3.

layer from the ground state. We found the ground state to be the C-AFM state and the averaged magnetic moment at the four edges of the C-AFM state to be 0.24 μ_B/atom, which is close to that of the monolayer ZGNR in the ground state (0.25 μ_B/atom). When ribbon widths, N are 4–9, 11, and 12, the C-AFM state was found to be the most stable. Figure 3 shows the band structures for magnetic states of the bilayer ZGNR. The FM and Ferri states are metallic, whereas the A-AFM, C-AFM, and G-AFM states are insulating. The C-AFM state has the largest band gap among these insulator structures. Figure 4 shows the spin density of the C-AFM state. The magnetic moments are localized at edges, as is the case for monolayer ZGNR. The magnetic stability is consistent with the size of the indirect band gap, as shown in Table I.

Next, we studied the carrier doped bilayer ZGNR. The calculation was performed by the Fermi-level shift (FLS) method, in which we introduced a uniform background charge so that the system was neutral. The number of doped carriers per ZGNR layer is expressed as x (e/layer), where positive and negative e values correspond to hole and electron doping, respectively. We calculated the total energy measured from the ground state for a given x. Figure 5 shows the total energy difference from the ground state per ZGNR layer as a function of x. The C-AFM state is the ground state in the regions of $-0.03\,e$/layer $< x < 0.03\,e$/layer. The FM state is the ground state in the regions of $x < -0.035\,e$/layer and $0.035 < x\,e$/layer. As $|x|$ increases, the exchange interaction changes from AFM to FM at intraplane-edge atoms, whereas the FM coupling is maintained between the interplane-edge atoms. A recent theoretical study using a tight-binding model in magnetic bilayer ZGNRs support our results for the stability of interplane FM interaction in the carrier-doped bilayer ZGNR.[21] This suggests that the interplane FM ordering is unchanged with respect to the carrier doping induced by impurities or lattice defects in the bilayer ZGNR. Moreover, it is expected that the spin-canted state would appear at the doping region where the magnetic
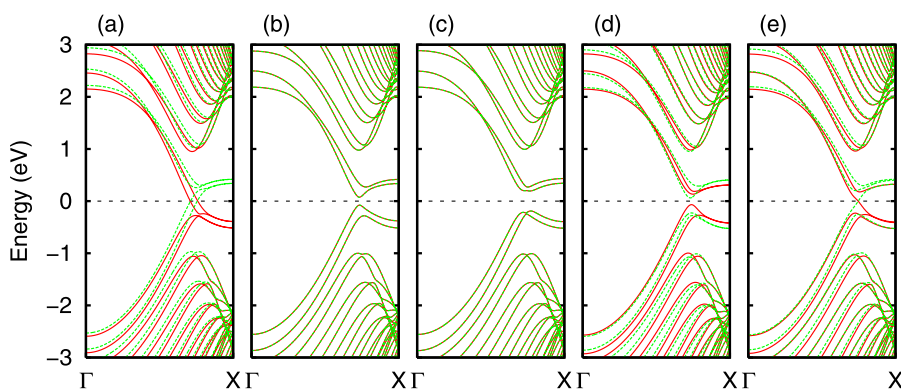
FIG. 3. Band structures of bilayer ZGNR. The Fermi level is located at $E_F = 0$. The solid and dashed lines indicate the up and down spin states, respectively. (a), (b), (c), (d), and (e) denote the FM, A-AFM, C-AFM, G-AFM, and Ferri states, respectively.
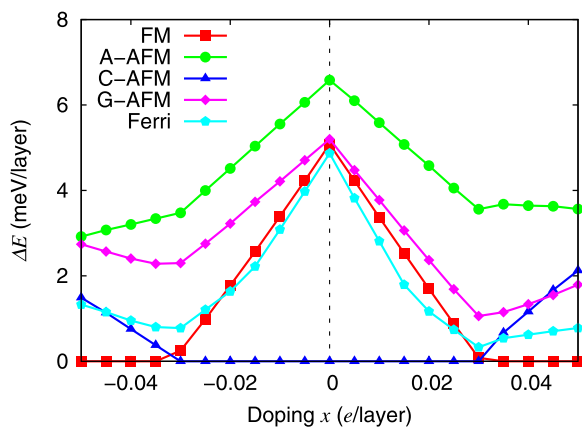
FIG. 5. The total energy difference per ZGNR layer from the ground state as a function of carrier concentration x. The red squares, green circles, blue triangles, pink diamonds, and light blue pentagons denote the FM, A-AFM, C-AFM, G-AFM, and Ferri states, respectively. The lines serve as a visual reference.

ground state nearly degenerates ($\sim$0.03 e/layer) as well as in the case of the monolayer ZGNR.[8]

Finally, we discuss the stability of the interplane FM coupling. When we varied the interlayer distance in the range of $3.2\,\text{Å} \leq d \leq 4.3\,\text{Å}$ under the condition that the atomic position of the x- and y-planes were fixed, We found that the C-AFM state is always the ground state. We studied the magnetic stability for the trilayer ZGNR and two-dimensional ZGNRs stacked periodically along the z-direction and found that the C-AFM state is the ground state in both cases. It is expected that the FM coupling between the inter-layer edge atoms is very robust under the various conditions. Therefore, it is suggested that the carrier-induced multilayer ZGNR becomes FM with large magnetization.

In summary, we have performed first-principles DFT cal-culations to clarify the magnetic stability of bilayer ZGNRs. We found that the magnetic ground state is the C-AFM state, which is the AFM order between intraplane-edge C atoms and the FM order between interplane-edge C atoms. The averaged magnetic moment of the edges was close to that of monolayer ZGNRs. For trilayer and multilayer ZGNRs, the C-AFM state was also the most stable. We found that the magnetic ground state changes from the C-AFM state to the FM state by carrier doping. We expect the carrier-doped infinitely stacked multi-layer ZGNR become two-dimensional ferromagnetic surface (edge) states of graphite with a metallic conductivity.

[1]N. Tombros, C. Jozsa, M. Popinciuc, H. T. Jonkman, and B. J. Van Wees, Nature **448**, 571 (2007).
[2]M. Ohishi, M. Shiraishi, R. Nouchi, T. Nozaki, T. Shinjo, and Y. Suzuki, Jpn. J. Appl. Phys., Part 2 **46**, L605 (2007).
[3]Y.-W. Son, M. L. Cohen, and S. G. Louie, Nature **444**, 347 (2006).
[4]E.-J. Kan, Z. Li, J. Yang, and J. G. Hou, J. Am. Chem. Soc. **130**, 4224 (2008).
[5]O. Hod, V. Barone, and G. E. Scuseria, Phys. Rev. B **77**, 035411 (2008).
[6]M. Fujita, K. Wakabayashi, K. Nakada, and K. Kusakabe, J. Phys. Soc. Jpn. **65**, 1920 (1996).
[7]K. Nakada, M. Fujita, G. Dresselhaus, and M. S. Dresselhaus, Phys. Rev. B **54**, 17954 (1996).
[8]K. Sawada, F. Ishii, M. Saito, S. Okada, and T. Kawai, Nano Lett. **9**, 269 (2009).
[9]K. Sawada, F. Ishii, and M. Saito, Appl. Phys. Express **1**, 064004 (2008).
[10]H. Lee, N. Park, Y.-W. Son, S. Han, and J. Yu, Chem. Phys. Lett. **398**, 207 (2004).
[11]H. Lee, Y.-W. Son, N. Park, S. Han, and J. Yu, Phys. Rev. B **72**, 174431 (2005).
[12]T. Ozaki, H. Kino, J. Yu, M. J. Han, N. Kobayashi, M. Ohfuti, F. Ishii, T. Ohwaki, H. Weng, and K. Terakura, OPENMX, version 3.5, a package of *ab initio* programs, 2009.
[13]J. P. Perdew, K. Burke, and M. Ernzerhof, Phys. Rev. Lett. **77**, 3865 (1996).
[14]N. Troullier and J. L. Martins, Phys. Rev. B **43**, 1993 (1991).
[15]T. Ozaki, Phys. Rev. B **67**, 155108 (2003).
[16]T. Ozaki and H. Kino, Phys. Rev. B **69**, 195113 (2004).
[17]A. D. Becke and R. M. Dickson, J. Chem. Phys. **89**, 2993 (1988).
[18]O. Chmaissem, B. Dabrowski, S. Kolesnik, J. Mais, J. D. Jorgensen, and S. Short, Phys. Rev. B **67**, 094431 (2003).
[19]Z. Fang, I. V. Solovyev, and K. Terakura, Phys. Rev. Lett. **84**, 3169 (2000).
[20]K. Sawada and F. Ishii, J. Phys.: Condens. Matter **21**, 064246 (2009).
[21]L. Pan, J. An, and Y.-J. Liu, New J. Phys. **15**, 043016 (2013).